Catal Lett (2008) 125:264–270
DOI 10.1007/s10562-008-9586-2

Fischer–Tropsch Synthesis Using Zeolite-supported Iron Catalysts for the Production of Light Hydrocarbons

Suk-Hwan Kang · Jong Wook Bae · P. S. Sai Prasad · Ki-Won Jun

Received: 28 April 2008 / Accepted: 9 July 2008 / Published online: 25 July 2008

Abstract Fischer–Tropsch synthesis (FTS) for the production of olefins from syngas was investigated on FeCuK impregnated on zeolite catalysts such as ZSM-5, Mordenite and Beta-zeolite. ZSM-5 supported catalyst showed the best activity among the three catalysts due to the high reducibility of iron oxides. It also exhibited high olefin selectivity compared to a catalyst prepared by physical mixing of the two components, due to the presence of moderate number of acid sites.

Keywords Fischer–Tropsch synthesis · Iron · Zeolites · Light hydrocarbons · Acidity

1 Introduction

The Fischer–Tropsch synthesis (FTS) has been recognized as an important alternate technology to petroleum refining in the production of liquid fuels and chemicals from syngas derived from coal, natural gas and other carbon-containing materials [1]. Fe-based catalyst is often selected for the FTS, over its competitor of Co-based catalyst, because of its WGS activity to work in a wide range of H_2/CO feed ratio [2, 3]. Further, iron is much less expensive than Co and has lower methane selectivity. However, many promoters have been used [4] to improve the CO hydrogenation functionality of Fe-based catalysts. For example, Cu as a reduction promoter helps decrease the reduction temperature of iron oxides. The component of SiO_2 as a structural promoter, helps increase the surface area as well as the attrition resistance of the catalysts that is particularly required for the slurry phase reaction. K is added frequently as a chemical promoter for providing a higher chain growth factor value, increasing the olefin/paraffin ratio in the hydrocarbon product and decreasing the catalyst deactivation rate. Supports such as Al_2O_3, TiO_2 and SiO_2 have been used to stabilize the active components as well.

The Fischer–Tropsch (FT) catalysts normally lead to a typical non-selective Anderson–Schulz–Flory (ASF) product distribution, limiting the selectivity of the required fraction. In order to provide high product selectivity [5], the usage of a bifunctional catalyst, consisting of a FT active metal and an acidic zeolite, has been the focus of attention recently. In this type of composite catalyst, the FT active metal transforms the syngas into the primary straight chain hydrocarbon product which, in turn, undergoes further restructuring on the acid component (co-catalyst) to produce a more branched and aromatic hydrocarbon products of limited chain length. Sulphated zirconia was selected initially as a co-catalyst in the FTS for the production of C_4 hydrocarbons [6]. However, due to carbon deposition and sulphate reduction, it quickly deactivated even at a very low level of CO conversion. Therefore, zeolite or metal/zeolite has been preferred for the second catalytic function. The composite catalysts can be prepared either by directly supporting the FT active metals on zeolites, application of zeolite as a membrane in the FT catalyst, synthesizing a hybrid catalyst consisting of the FT catalyst and a zeolite or metal/zeolite catalyst, or by using dual beds, one containing the FT catalyst and the other a zeolite catalyst [7].

Mobil Oil workers initially conducted much work on the iron/ZSM-5 bifunctional catalyst and found that the acid catalyst deactivated very rapidly compared to the iron catalyst and that it was not effective in the low temperature

S.-H. Kang · J. W. Bae · P. S. Sai Prasad · K.-W. Jun (✉)
Alternative Chemicals/Fuel Research Center, Korea Research Institute of Chemical Technology (KRICT), P.O. Box 107, Yusong, Daejon 305-600, South Korea
e-mail: kwjun@krict.re.kr

range (230–260 °C) where bifunctional catalysis is needed. Sasol workers, on the other hand, operating their iron catalyst at high temperature (330–350 °C) produced essentially no products above C_{20} as the catalyst particles agglomerated with the wax and finally found a difficulty in fluidization. Studies at intermediate temperatures are scarce.

In contrast to the Co based catalysts, in the case of iron based composite catalysts, most of the researchers have preferred using a physical mixture of the iron component and the zeolite to understand the influence of nature of zeolite on the activity and product selectivity. Studies of the impregnated catalysts are scarce [8–12], particularly aiming at maximizing the light olefin yield. In this presentation, we report the olefin synthesis from syngas over the catalysts containing Fe–Cu–K supported on different zeolites. These composite catalysts were prepared by the conventional impregnation technique. The objective of this work is to find the influence of the pore structure and the acidity of the zeolites on its performance in the FTS from syngas. The properties of the catalysts are further substantiated by using the characterization tools such as surface area measurement, XRD, TPR and NH_3-TPD.

2 Experimental

2.1 Catalyst Preparation

The Fe-based catalysts for FTS from syngas were prepared by the conventional wet-impregnation of the proton-type zeolites, namely ZSM-5 (Si/Al = 25, surface area = 425 m^2/g), Mordenite (Si/Al = 6, surface area = 420 m^2/g) and Beta-zeolite (Si/Al = 12.5, surface area = 680 m^2/g) with the salts or the active component. Aqueous iron nitrate, copper nitrate and potassium carbonate solutions, in required composition, were mixed thoroughly. The impregnation on the zeolites was carried out with continuous stirring at 60 °C for 6 h. The samples were then dried in a rotary evaporator before subjecting them for calcination at 500 °C in air for 5 h. The ratio of iron metal component to that of the zeolite in the finished catalyst was fixed at 20/100 by weight percentage and the Fe/Cu/K ratio as 20/2/4 by weight.

2.2 Characterization

BET surface area and BJH pore size distribution of the hybrid catalysts were determined by N_2-physisorption using Micromeritics ASAP 2400 apparatus at liquid-N_2 temperature at −196 °C. The acidity of the catalysts was measured by the temperature-programmed desorption of ammonia (NH_3-TPD). Before the analysis, about 0.10 g of the sample was pretreated at 250 °C in a flow of helium for 2 h to remove the physisorbed water. After cooling to room temperature, ammonia was introduced into the reactor at 100 °C for 1 h and the physisorbed ammonia was removed in a helium flow at 100 °C for about 30 min. Subsequently, the sample was heated from 100 °C to 800 °C, with a ramping rate of 10 °C/min and kept at the same temperature for 30 min in a flow of helium gas. The effluent gas was analyzed by an on-line gas chromatograph with a TCD detector. The powder X-ray diffraction (XRD) patterns were obtained with a Rigaku diffractometer using Cu-K_α radiation to identify the phases of FeCuK/zeolite catalysts. The temperature programmed reduction (TPR) experiments were performed to determine the reducibility of the surface oxides. Prior to the TPR experiments, the samples were pretreated in a He flow up to 400 °C and kept for 2 h to remove the adsorbed water and other contaminants followed by cooling to 50 °C. The reducing gas containing 5% H_2/Ar mixture was passed over the samples at a flow rate of 30 mL/min, with the heating rate of 10 °C/min up to 800 °C and kept at that temperature for 30 min.

2.3 Activity Test

Catalytic activity test was carried out in a tubular fixed bed reactor (O.D. = 12.7 mm) with a catalyst of 0.3 g. Prior to the reaction, the catalyst was reduced at 450 °C for 12 h in a flow of 5% H_2 balanced with nitrogen. After reduction, the synthesis gas (H_2/CO = 2) was fed into the reactor. The FTS reaction was carried out subsequently under the following reaction conditions; T = 300 °C, P = 1.0 MPa and SV = 2,000 mL/g_{cat} h. Effluent gas from the reactor was analyzed by an online gas chromatograph (YoungLin Acme 6000 GC) employing GS-GASPRO capillary column connected with FID for the analysis of hydrocarbons and Porapak Q/molecular sieve (5A) packed column connected with TCD for the analysis of carbon oxides, hydrogen, methane and internal standard gas (Ar).

3 Results and Discussion

3.1 Textural Properties of the Fresh Catalysts

Because of their molecular sieve as well as shape selective character, zeolites have been used as supports, instead of oxides, for several catalysts. Zeolites are particularly used as acidic catalysts, as the concentration and the strength of the acid sites are controllable [13], and to exploit their regular pore structure. Thus, the three zeolites which differ in their dimensionality and acidity, were selected to elucidate the influence of these parameters on the activities and selectivities of the composite catalysts on FTS.

The three zeolites used have different pore structure and surface properties. ZSM-5 is a medium-pore zeolite that contains two intersecting channel systems. The elliptical 10-member ring (MR) openings controlling the channels have an effective diameter of ca. 0.56 nm [14]. Mordenite possesses 12-MR straight pore channel and a wide pore entrance. Beta-zeolite has a tridirectional system of interconnected channels. The textural properties, like BET surface area, pore volume and average pore diameter of the catalysts prepared using these supports are summarized in Table 1 and their pore size distribution patterns are shown in Fig. 1. In the present study, the composite catalyst of FeCuK/Beta-zeolite is found to contain mainly mesopores around 30 nm with a maximum peak intensity for dV/dlog(D), whereas the other two catalysts exhibit the presence of micropores around 4 nm, after loading with the active component. The decrease in the surface area of the zeolites after impregnation and calcination are 38%, 85% and 45% in the case of ZSM-5, Mordenite and Beta-zeolite supported catalysts, respectively. Broadly, these values depict a fairly uniform distribution of the active component (26 wt.%) inside the zeolite in the case of ZSM-5, a substantial pore filling in the case of Mordenite and a moderate distribution in the case of Beta-zeolite.

Table 1 Textural properties of FeCuK/zeolite catalysts

Notation	BET surface area (m^2/g)	Pore volume (cm^3/g)	Average pore diameter (nm)	Si/Al ratio
FeCuK/ZSM-5	265 (425)[a]	0.112	11.9	25
FeCuK/ Mordenite	64 (420)	0.059	14.8	6
FeCuK/ Beta-zeolite	372 (680)	0.550	17.4	12.5

[a] The values in the parentheses correspond to that of the support

3.2 Temperature-programmed Analysis (H_2-TPR and NH_3-TPD)

The effect of the nature of zeolite on the ease of reduction was investigated by H_2-TPR. Figure 2 shows the H_2-TPR profiles of the catalysts with different zeolites used as supports. As most of the copper promoted iron-based catalysts, the reduction process in H_2 occurs in two distinct stages. The first stage, occurring between 200 °C and 350 °C, corresponds to the combined reduction of Fe_2O_3 to Fe_3O_4 and CuO to Cu. The second stage, at the high temperature region of 350–800 °C, represents the reduction of Fe_3O_4 to Fe metal. In the case of FeCuK/Beta-zeolite, the first peak itself is split into two; the CuO reduction appearing first as a discrete peak and the second one representing the reduction of Fe_2O_3 to Fe_3O_4. The appearance of a separate peak for CuO reduction implies a non-homogeneous mixing of Cu and Fe species and hence Cu could not promote efficiently the reduction of iron. Consequently, there appears a large high temperature peak in the case of Beta-zeolite supported catalyst. This argument is in line with the observations of Wu et al. [15]. A well-mixed system can be assumed in the case of ZSM-5 supported catalyst wherein the first peak has no shoulder and is of higher intensity. As has been reported frequently, CuO facilitates the reduction of α-Fe_2O_3 when the two phases are well mixed, resulting in the corresponding peaks appearing at much lower temperature [16]. The second stage represents the transformation of $Fe_3O_4 \rightarrow \alpha$-Fe. Shen et al. [17] have used precipitated FeCuK in combination with ZSM-5 zeolite for the preparation of gasoline and also

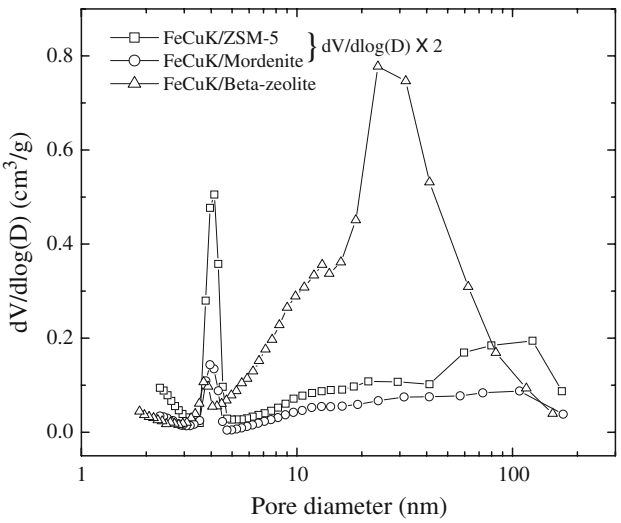

Fig. 1 Pore size distribution of the FeCuK/zeolite catalysts

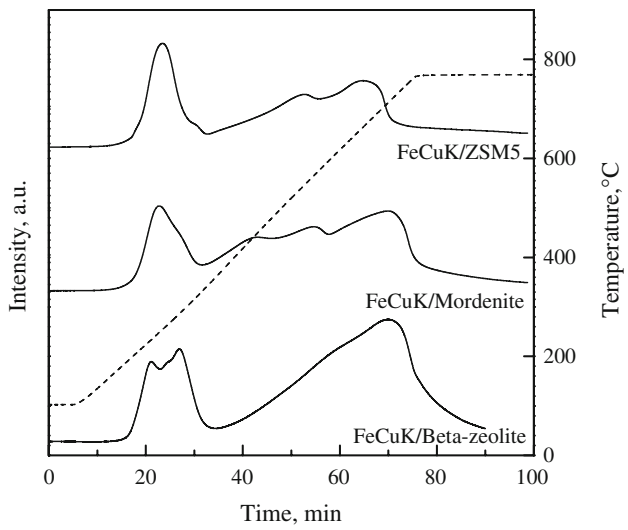

Fig. 2 H_2-TPR profiles of the fresh FeCuK/zeolite catalysts

found Cu promotion to decrease the iron reduction temperature as well as the operation temperature and stabilize the activity and selectivity.

The degree of reduction of the composite catalysts was calculated from the hydrogen consumption values of TPR runs. The reduction degree was expressed as the ratio of the hydrogen consumed below 450 °C to the total hydrogen consumed during the TPR of the fresh catalyst. The values expressed as percentages are 39.6%, 36.2% and 31.3% for FeCuK/ZSM-5, FeCuK/Mordenite and FeCuK/Beta-zeolite, respectively. These results are in accordance with the apparent degree of mixing of Cu and Fe species in the catalysts.

The NH_3-TPD patterns of the FT catalysts are shown in Fig. 3. A two- or three-stage desorption of NH_3 is observed. The desorption peaks observed at 350–550 °C are attributed to strong acid sites, whereas those at 150–300 °C to weak acid sites or physically adsorbed ammonia [18]. Table 2 gives the number of acid sites expressed as mmol NH_3/g of catalyst. It can be observed that the number of acid sites is the highest for FeCuK/Mordenite, in both first and second (and third temperature) regions. Further, the total number of acid sites varies in the order of FeCuK/Mordenite > FeCuK/Beta-zeolite > FeCuK/ZSM-5. As a coincidence, the acidity decreases proportionately with the increase in Si/Al ratio of the zeolite supports, indicating that the effect of impregnation is uniform in all the supports.

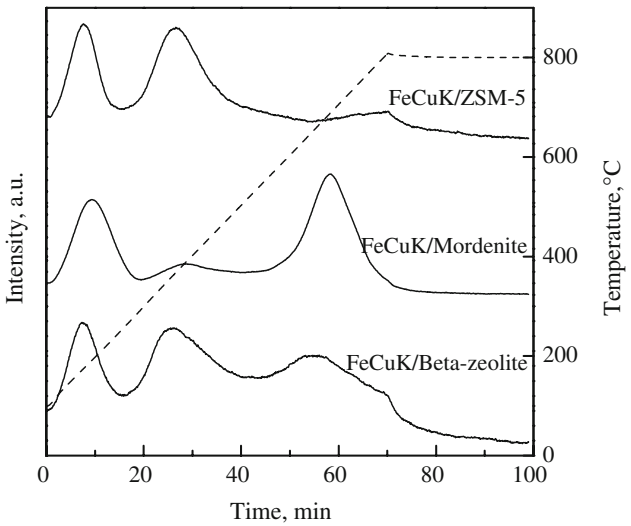

Fig. 3 NH_3-TPD profiles of the FeCuK/zeolite catalysts

Table 2 Surface acidity of FeCuK/zeolite catalysts measured by NH_3-TPD

Notation	Acidic site (mmol NH_3/g)		
	First	Second (and third)	Total
FeCuK/ZSM-5	0.096	0.170	0.266
FeCuK/Mordenite	0.364	0.755	1.119
FeCuK/Beta-zeolite	0.098	0.358	0.456

3.3 FTS Activity of the Composite Catalysts

The catalytic performance of the FeCuK/zeolite catalysts was measured at 300 °C, 1.0 MPa, 2,000 mL/g_{cat} h and $H_2/CO = 2$. The activity of catalysts was tested for over 120 h. Figure 4 shows the variation in conversion with time on stream (TOS) and the relative stability of the catalysts, activity being expressed in terms of percentage conversion of CO. The conversion of CO observed for FeCuK/ZSM-5 and FeCuK/Beta-zeolite catalysts increases slowly with time on stream, whereas that for FeCuK/Mordenite catalyst rapidly reaches a maximum at the early stages of the reaction and then decreases slowly with time on stream. The activity of the catalysts (after a TOS of 120 h) varies in the order FeCuK/ZSM-5 > FeCuK/Mordenite > FeCuK/Beta-zeolite. In the case of Mordenite possessing a two-dimensional pore structure the activity decreases with time on stream due to a possible increase in coke formation. A considerable decrease in surface area due to pore filling also supports this observation, as catalysts with larger pores resist deactivation. In this respect supports with a three-dimensional pore structure, (ZSM-5 and Beta-zeolite), seem to be beneficial.

Fe catalysts show high water-gas shift (WGS) activity, and hence are of increasing interest for FTS than the Co-based catalysts. A great number of studies [15] have focused on the phase transformation and on identifying the catalytically active phases during the FT reaction over the iron catalysts. Fe carbides, Fe_3O_4, Fe metal, or surface iron phases on Fe_3O_4 have been proposed to be the active species for FT reaction by different researchers [19]. The nature of

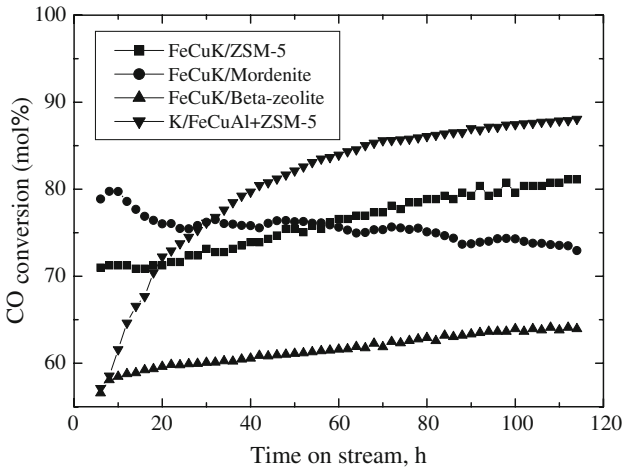

Fig. 4 Activity variation of the FeCuK/zeolite catalysts with time on stream

the active site depends on the reaction conditions [20]. A lot of discussion has gone into establishing the carbide as the active species [21] as CO dissociation occurs on these sites. Further, Sudsakorn et al. [22] have suggested formation of similar nature of active sites even when the Fe catalysts are activated differently (using H_2, CO or syngas, respectively). Literature reveals a direct evidence for a possible relationship between the catalytic activity and the formation of iron carbides [21]. In the present investigation, FeCuK/ZSM-5 has exhibited the highest activity (after 120 h of time on stream) followed by Mordenite and Beta-zeolite supported catalysts. This can be explained in terms of ease of reduction, as seen by the TPR patterns given in Fig. 2. The higher the reducibility of the iron species, the more the number of carbide species that can be formed. FeCuK/ZSM-5, which records the highest reducibility, shows the maximum conversion followed by the Mordenite and the Beta-zeolite based catalysts. In the case of physically mixed catalysts, the advantage of the bifunctional catalyst has been explained in terms of changing the adsorption–desorption equilibrium of olefins on the iron phase [23]. However, the validity of this assumption in the case of impregnated catalysts needs to be examined.

In order to understand further, the reason for change in the activity of the three zeolite supported catalysts, a detailed XRD study was carried out on the catalysts. Figure 5 displays the XRD patterns of the catalysts before and after the reaction. The fresh catalysts have exhibited well-defined characteristic peaks of the respective zeolites. Apart from this, the major detectable iron phase of the catalysts is hematite (α-Fe_2O_3), with the characteristic peaks appearing at 2θ values of 24.2°, 33.1°, 35.6°, 40.8°, 49.5°, 54.0°, 57.6°, 62.5° and 64.0°, and agreeing with data reported in the JCPDS files. The XRD patterns of the catalyst samples, collected after around 120 h of reaction, show peaks of iron carbide and metallic iron. Particularly, the broad peak at 44° is a strong indication for the carbide formation, as also reported by Ning et al. [24]. However, the sharpness of the zeolite peaks disappeared and in their place some very broad peaks have been observed. It appears that the catalysts were disintegrated, at least partially, during the reaction. This may be due to coagulation of iron moieties prepared by impregnation, with a consequent increase in cell volume than that of the original zeolite, as reported by El Bahy et al. [25]. The situation is better in the case of ZSM-5 supported system in the present case, wherein some of the diffraction lines are clearly visible. Thus, the degradation of the structure of the zeolites might have led to formation of interacted species between iron and alumina (or silica) further decreasing the reducibility of iron in the case of Mordenite and Beta-zeolite supported catalysts.

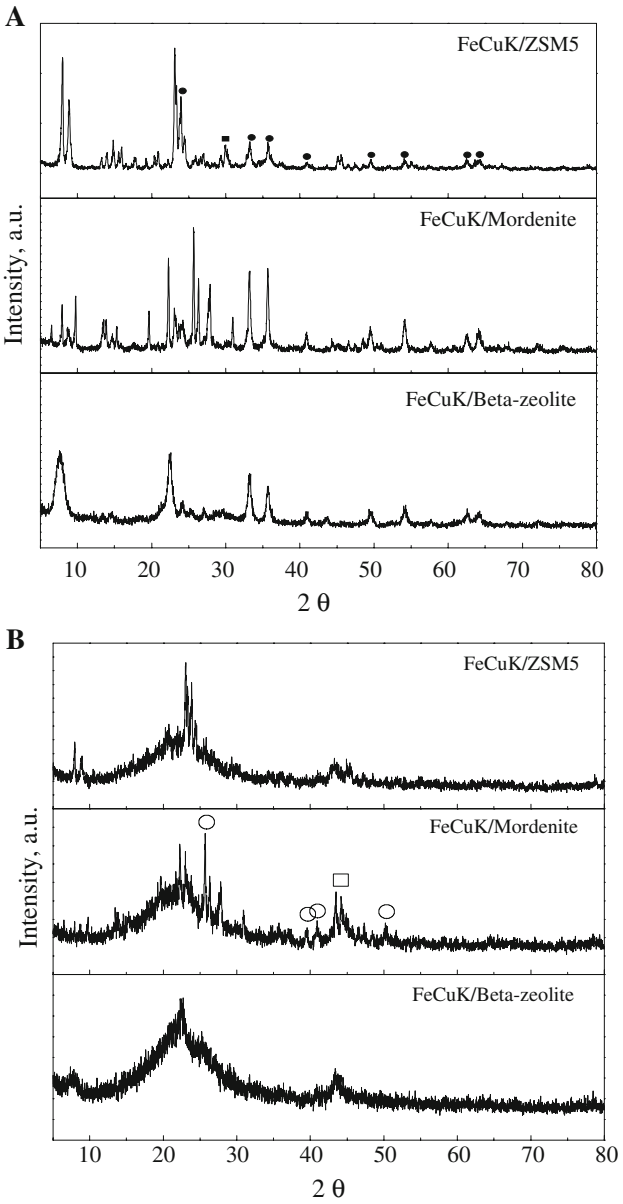

Fig. 5 XRD patterns of the FeCuK/zeolite catalysts; (**a**) before reaction (■ α-Fe_2O_3, ● γ-Fe_2O_3) and (**b**) after FTS reaction for around 120 h (□ Fe, ○ FeC_X)

3.4 Comparison of the Product Distributions Obtained on the Impregnated and Physically Mixed Catalysts

Table 3 displays the product distribution including the yield of olefins in the range of C_2–C_4 hydrocarbons obtained on the three catalysts. FeCuK/ZSM-5 shows the highest selectivity (71.2%) towards the olefins. The Mordenite based catalyst has the lowest percentage O/(O + P) of 42.5%. FeCuK/Beta-zeolite shows the intermediate value. The existence of stronger acid sites on Mordenite supported catalyst (Table 2) can be the reason for suppressed olefin formation. This observation is in accordance with that of

Table 3 CO hydrogenation[a] over FeCuK/zeolite catalysts

	FeCuK/ZSM-5	FeCuK/Mordenite	FeCuK/Beta-zeolite	K/FeCuAl + ZSM-5
CO Conv. (%)	81.1	72.9	63.9	88.1
Selectivity (C mol%)				
CO_2	35.6	37.7	25.2	45.1
–HC–[b]	64.4	62.3	74.8	54.9
Hydrocarbon distribution (C mol%)				
C1	19.6	32.2	31.5	19.5
C2=	4.2	1.9	3.7	0.7
C2	6.5	13.1	11.8	6.4
C3=	13.4	8.2	13.8	0.8
C3	2.9	8.2	5.7	7.5
C4=	12.7	8.7	11.7	9.5
C4	2.9	4.1	4.1	15.0
C5>	37.8	23.6	17.7	40.6
Olefins in (C_2–C_4) (C mol%)				
Selectivity: O/(O + P)[c]	71.2	42.5	57.6	27.7
% yield[d]	13.8	6.6	11.3	4.7

[a] CO hydrogenation at $H_2/CO = 2$, SV = 2,000 ml/g h, T = 300 °C and P = 1.0 MPa

[b] Hydrocarbon selectivity

[c] Olefin-to-paraffin ratio in the range of C_2–C_4 hydrocarbons

[d] CO mol% transformed to olefins in the range of C_2–C_4 hydrocarbons

Basu et al. [27]. Hammer et al. [28] have investigated the role of ZSM-5, Mordenite and Beta-zeolites in combined with Fe (promoted with Cu and K). They have identified the product composition to be significantly different from that of classical straight-chain FTS products. The products contained more isomers, olefins and oxygenates due to the different acidity of the zeolites. The acidic catalyst promotes the formation of isomers and aromatics in the gasoline range with a maximum chain length of C_{12} at the expense of olefins [29], thus reducing the O/(O + P) ratio, as it has less number of strong acid sites. The decrease in selectivity and yield of olefins with increase in acidity, shown in Fig. 6 also reiterates this observation. ZSM-5 seems to be a better support for obtaining higher O/(O + P) ratio. ZSM-5 has also been a particularly preferred zeolite support for bifunctional catalysts, as it limits the growth of chain length to gasoline range hydrocarbons in the case of methanol conversion [14].

It can be observed from Table 3 that the methane composition in the hydrocarbon fraction of the product is lower in the case of ZSM-5 based catalyst than that of the other catalysts. Methane formation occurs due to cracking of hydrocarbons over acidic sites on the zeolites. The acidity of the zeolites and the reaction conditions decide about the extent of methane formation. Under similar reaction conditions, the methane selectivity, as shown in Table 3, decreased in the order FeCuK/Mordenite > FeCuK/Beta-zeolite > FeCuK/ZSM-5. This is consistent with the decrease in the acidity of the catalysts, as also reported in the literature [30]. It can be seen from the TPR patterns that the reducibility of iron oxides in ZSM-5 supported catalyst is high and hence is expected to have less number of non-carbidic sites. Therefore, its methane formation is expected to be low. The ZSM-5 based catalyst has recorded a higher selectivity to CO_2 compared to that of the Beta-zeolite based catalyst. In the FTS reaction, CO_2 is a product of water gas shift reaction and iron catalysts are known for their high WGS shift activity as well. Therefore, when the catalyst is active for CO hydrogenation it can be expected that WGS is

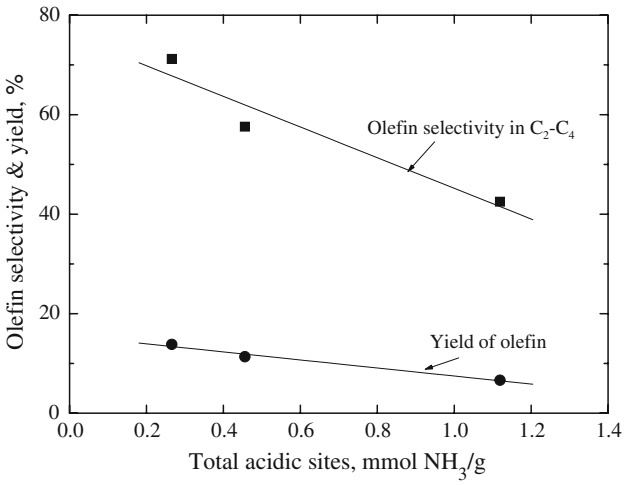

Fig. 6 A correlation between the acidity and the yield of olefins in the range of C_2–C_4 hydrocarbons

also favorable before reaching the equilibrium conversion between CO and CO_2.

Table 3 also discloses the activity and selectivity obtained on a model catalyst, FeCuKAl + ZSM-5 zeolite prepared by physical mixing of the metallic and acidic components. The preparation method of precipitated FeCuKAl and its FTS activity was investigated already in our previous works by using the biomass-derived syngas [31]. The role of alumina can be neglected as it is used as a binder, not to influence much on the reducibility and acidic properties of the catalyst. A comparison of the performance of the impregnated catalyst FeCuK/ZSM-5 with that of the above catalyst reveals that in spite of slightly lower CO conversion, the impregnated catalyst offers better selectivity towards the olefins. As can be seen from Fig. 4, the impregnated and the physically mixed catalysts show variation in their activity pattern. The conversion curve started with a very low value and showed an increasing trend with time on stream on the physically mixed catalysts. The impregnated catalysts, on the other hand, showed higher initial activity with variation with time on stream. This difference in the activity patterns could be explained due to the phenomenon of dispersion of the active component in the case of impregnated catalysts. An additional evaluation run conducted under the same conditions, on the FeCuKAl bulk catalyst (without the support) revealed higher conversion (90%), higher selectivity towards CO_2 (36.6%) and lower selectivity to methane (4.6%) but with much lower yield of olefins when compared with that of FeCuK/ZSM-5 catalyst. Further detailed investigations are in progress to explain clearly the difference in the performance of the catalysts.

4 Conclusions

Among the three zeolites selected as supports to impregnate FeCuK mixture on them, ZSM-5 seems to be the best as it retains the physical structure and allows higher reduction of iron species. Mordenite and Beta-zeolite lost their structure during the reaction. The conversion of CO on FeCuK/ZSM-5 is found to be the highest as more number of carbide species could be formed. It also offers higher olefin selectivity due to moderate acidity, not allowing the olefins for further transformations. A comparison of the activity and selectivity of the impregnated catalyst with that of the physically mixed catalyst shows higher olefin selectivity, in spite of slightly lower activity.

Acknowledgments The authors would like to acknowledge funding from the Korea Ministry of Knowledge Economy (MKE) through ''Project of next-generation novel technology development'' of ITEP. P.S. Sai Prasad thanks Korea Federation of Science & Technology (KOFST) for the award of the visiting research fellowship under Brain Pool program.

References

1. Zhang CH, Yang Y, Tenga BT, Li TZ, Zheng HY, Xiang HW, Li YW (2006) J Catal 237:405
2. Jothimurugesan K, Goodwin Jr JG, Gangwal SK (2004) US Patent 0220437 A1
3. Espinoza RL, Jothimurugesan K, Raje AP (2006) US Patent 7067562 B2
4. Lohitharn N, Goodwin JG Jr, Lotero E (2008) J Catal 255:104
5. Bartholomew CH (1991) Stud Surf Sci Catal 64:158
6. Sethuraman R, Bakhshi NN, Katikaneni SP, Idem RO (2001) Fuel Proc Technol 73:197
7. Liu ZW, Li X, Asami K, Fujimoto K (2007) Fuel Proc Technol 88:165
8. Chang CD, Lang WH, Silvestre AJ (1979) J Catal 56:268
9. Udaya V, Rao S, Gormley RJ (1990) Catal Today 6:207
10. Nguyen-Ngoc H, Moller K, Ralea M (1984) Stud Surf Sci Catal 18:291
11. Guan N, Liu Y, Zhang M (1996) Catal Today 30:207
12. Botes FG, Böhringer W (2004) Appl Catal A 267:217
13. Guczi L, Kiricsi I (1999) Appl Catal A186:375
14. Martínez A, Rollán J, Arribas MA, Cerqueira HS, Costa AF, Falabella E, Aguiar S (2007) J Catal 249:162
15. Wu B, Tian L, Xiang H, Zhang Z, Li YW (2005) Catal Lett 102:211
16. Ereña J, Garoña R, Arandes JM, Aguayo AT, Bilbao J (2005) Catal Today 107–108:467
17. Shen WJ, Chen SS, Yu-Long Z, Lai J, Zhang BJ (1995) J Nat Gas Chem 4:374
18. Lónyi F, Valyon J (2001) Microporous Mesoporous Mat 47:293
19. Mansker LD, Jin Y, Bukur DB, Datye AK (1999) Appl Catal A 186:277
20. Huang CS, Xu L, Davis BH (1993) Fuel Sci Technol Int 11:6
21. Bian G, Oonnuki A, Koizumi N, Nomoto H, Yamada M (2002) J Mol Catal A 186:203
22. Sudsakorn K, Goodwin JG, Adeyiga AA (2003) J Catal 213:204
23. Machocki A, Chmiel B (2006) Ann Univ Mariae Curie-Sklodowska Sect AA: Chemia 61:153
24. Ning W, Koizumi N, Chang H, Mochizuki T, Itoh T, Yamada M (2006) Appl Catal A 312:35
25. El-Bahy ZM, Mohamed MM, Zidan FI, Thabet MS (2008) J Hazard Mater 153:364
26. Wagner CD, Riggs WM, Davis LE, Moulder JF, Muilenberg GE (eds) (1978) Handbook of X-ray photoelectron spectroscopy. Perkin-Elmer, Minnesota
27. Basu PK, Roy SK, Sarkar PK, Ray SK, Krishnamurthy VA (1991) Fuel Sci Technol 10:91
28. Hammer H, Joisten M, Luengen S, Winkler D (1994) Inter J Energy Res 18:223
29. Egiebor NO, Cooper WC, Wojciechowski BW (1989) Appl Catal 55:47
30. Jiang G, Zhang L, Zhao Z, Zhou X, Duan A, Xu C, Gao J (2008) Appl Catal A 340:176
31. Jun KW, Roh HS, Kim KS, Ryu JS, Lee KW (2004) Appl Catal A 259:221